

# Monomeric Sarcosine Oxidase: 1. Flavin Reactivity and Active Site Binding Determinants<sup>†,‡</sup>

Mary Ann Wagner,<sup>§</sup> Peter Trickey,<sup>||</sup> Zhi-wei Chen,<sup>||</sup> F. Scott Mathews,<sup>||</sup> and Marilyn Schuman Jorns<sup>\*,§</sup>

Department of Biochemistry, MCP Hahnemann School of Medicine, Philadelphia, Pennsylvania 19129 and Department of Biochemistry and Molecular Biophysics, Washington University School of Medicine, St. Louis, Missouri 63110

Received February 15, 2000; Revised Manuscript Received April 21, 2000

**ABSTRACT:** Monomeric sarcosine oxidase (MSOX) is an inducible bacterial flavoenzyme that catalyzes the oxidative demethylation of sarcosine (*N*-methylglycine) and contains covalently bound FAD [ $\alpha$ -(*S*-cysteinyl)FAD]. This paper describes the spectroscopic and thermodynamic properties of MSOX as well as the X-ray crystallographic characterization of three new enzyme-inhibitor complexes. MSOX stabilizes the anionic form of the oxidized flavin ( $pK_a = 8.3$  versus 10.4 with free FAD), forms a thermodynamically stable flavin radical, and stabilizes the anionic form of the radical ( $pK_a < 6$  versus  $pK_a = 8.3$  with free FAD). MSOX forms a covalent flavin-sulfite complex, but there appears to be a significant kinetic barrier against complex formation. Active site binding determinants were probed in thermodynamic studies with various substrate analogues whose binding was found to perturb the flavin absorption spectrum and inhibit MSOX activity. The carboxyl group of sarcosine is essential for binding since none is observed with simple amines. The amino group of sarcosine is not essential, but binding affinity depends on the nature of the substitution ( $\text{CH}_3\text{XCH}_2\text{CO}_2^-$ ,  $\text{X} = \text{CH}_2 < \text{O} < \text{S} < \text{Se} < \text{Te}$ ), an effect which has been attributed to differences in the strength of donor- $\pi$  interactions. MSOX probably binds the zwitterionic form of sarcosine, as judged by the spectrally similar complexes formed with dimethylthioacetate [ $(\text{CH}_3)_2\text{S}^+\text{CH}_2\text{CO}_2^-$ ] and dimethylglycine ( $K_d = 20.5$  and 17.4 mM, respectively) and by the crystal structure of the latter. The methyl group of sarcosine is not essential but does contribute to binding affinity. The methyl group contribution varied from  $-3.79$  to  $-0.65$  kcal/mol with  $\text{CH}_3\text{XCH}_2\text{CO}_2^-$  depending on the nature of the heteroatom ( $\text{NH}_2^+ > \text{O} > \text{S}$ ) and appeared to be inversely correlated with heteroatom electron density. Charge-transfer complexes are formed with MSOX and  $\text{CH}_3\text{XCH}_2\text{CO}_2^-$  when  $\text{X} = \text{S}$ ,  $\text{Se}$ , or  $\text{Te}$ . An excellent linear correlation is observed between the energy of the charge transfer bands and the one-electron reduction potentials of the ligands. The presence of a sulfur, selenium, or tellurium atom identically positioned with respect to the flavin ring is confirmed by X-ray crystallography, although the increased atomic radius of  $\text{S} < \text{Se} < \text{Te}$  appears to simultaneously favor an alternate binding position for the heavier atoms. Although L-proline is a poor substrate, aromatic heterocyclic carboxylates containing a five-membered ring and various heteroatoms ( $\text{X} = \text{NH}$ ,  $\text{O}$ ,  $\text{S}$ ) are good ligands ( $K_{d, \text{X}=\text{NH}} = 1.37$  mM) and form charge-transfer complexes with MSOX. The energy of the charge-transfer bands ( $\text{S} > \text{O} \gg \text{NH}$ ) is linearly correlated with the one-electron ionization potentials of the corresponding heterocyclic rings.

Monomeric sarcosine oxidase (MSOX)<sup>1</sup> catalyzes the oxidative demethylation of sarcosine (*N*-methylglycine) to yield glycine, formaldehyde, and hydrogen peroxide. Sarcosine is

a common soil metabolite that can act as sole source of carbon and energy for many microorganisms. MSOX is expressed as an inducible enzyme in many soil bacteria upon growth with sarcosine as source of carbon and energy (1). MSOXs from various sources are found to contain covalently bound FAD (2). Studies with MSOX from *Bacillus sp. B-0618* show that the covalent FAD [ $\alpha$ -(*S*-cysteinyl)FAD] is attached to a cysteine residue near the COOH-terminus of the protein ( $M_r = 43\,834$ ) (3).

MSOX is a member of a recently recognized family of prokaryotic and eukaryotic enzymes that catalyze similar oxidation reactions with various secondary amino acids and contain covalently bound flavin (3–5). MSOX, *N*-methyltryptophan oxidase, and pipecolate oxidase are all monomeric proteins (42–44 kDa). MSOX shares 43% sequence identity with *N*-methyltryptophan oxidase, an *E. coli* enzyme

<sup>†</sup> This work was supported in part by Grants GM 31704 (M.S.J.) and GM20530 (F.S.M.) from the National Institutes of Health.

<sup>‡</sup> Crystallographic coordinates have been deposited in the Protein Data Bank under the file names 1EL5, 1EL7, 1EL8, 1EL9, and 1ELi.

<sup>\*</sup> To whom correspondence should be addressed. Phone: (215) 991-8580; fax: (215) 843-8849; e-mail: marilyn.jorns@drexel.edu.

<sup>§</sup> MCP Hahnemann School of Medicine.

<sup>||</sup> Washington University School of Medicine.

<sup>1</sup> Abbreviations: DMG, dimethylglycine; MSOX, monomeric sarcosine oxidase; MSEA, methylselenoacetate; MTA, methylthioacetate; MTEA, methyltelluroacetate; NCS, noncrystallographic symmetry; PCA, pyrrole-2-carboxylate; TSOX, heterotetrameric sarcosine oxidase; FAD, flavin adenine dinucleotide; FMN, flavin adenine mononucleotide; EDTA, ethylenediaminetetraacetic acid;  $\text{NAD}^+$ , nicotinamide adenine dinucleotide; IP, ionization potential; RMSD, root-mean-square deviation.

of unknown metabolic function that contains the same covalent flavin [ $8\alpha$ -(*S*-cysteinyl)FAD] found in MSOX (3). MSOX exhibits 30% identity with pipecolate oxidase, a mammalian enzyme that plays a significant role in brain metabolism where L-pipecolate acts as a neuromodulator. Heterotetrameric sarcosine oxidase (TSOX) is an inducible bacterial enzyme important in sarcosine catabolism, similar to MSOX. TSOX contains four different subunits and three different coenzymes (FAD,  $\text{NAD}^+$ , covalently bound FMN). The  $\beta$ -subunit of TSOX (44 kDa) contains covalently bound FMN [ $8\alpha$ -( $\text{N}^3$ -histidyl)FMN] and exhibits 23% sequence identity with MSOX (4, 6).

The crystal structure of MSOX and its complexes with two inhibitors, methylthioacetate (MTA) and pyrrole-2-carboxylate (PCA), was recently solved at 2-Å resolution (7). MSOX is a two-domain protein with the covalent FAD bound in an extended conformation. The flavin domain binds the ADP portion of FAD. The "catalytic" domain contains Cys315, the covalent flavin attachment site. The flavin ring is bound at the bottom of a cleft between the flavin and catalytic domains in a highly basic environment that contains no acidic residues, only neutral and basic residues. The MSOX active site is located above the *re* face of the flavin ring. Putative catalytic residues are contributed by both domains and are highly conserved within the various members of the MSOX family.

In this paper, we describe studies with MSOX from *Bacillus sp. B-0618* that characterize the reactivity of the flavin ring and probe active site binding determinants. We also present the crystal structures of three new enzyme-inhibitor complexes of MSOX, two of which show intense charge-transfer bands with the flavin and the third being a tertiary amine that is not oxidized by MSOX. Correlations between flavin reactivity and active site binding determinants with the structure of the MSOX active site are discussed.

## EXPERIMENTAL PROCEDURES

**Materials.** Glucose oxidase (*Aspergillus niger*, Type V-S) benzoic acid, *N,N'*-dimethylglycine (DMG), 2-furoic acid, methyl viologen, thioglycolic acid, horseradish peroxidase, *o*-dianisidine, and pyrrole-2-carboxylate (PCA) were purchased from Sigma. Sarcosine, methoxyacetic acid, sodium butyrate, thiophene-2-carboxylic acid, methylthioacetic acid, and ethylmethylamine were obtained from Aldrich. Glycolic acid was from Baker. Glycine was from BioRad. Sodium sulfite was from Fluka. 5-Deazariboflavin was synthesized as previously described (8). The potassium salts of methylselenoacetate (MSEA) and methyltelluroacetate (MTEA) were generous gifts from Dr. Louis Silks [National Stable Isotope Resource at Los Alamos and NIH Supported Resource (RR02231)]. Dimethylthioacetic acid [ $\text{CH}_3)_2\text{S}^+\text{CH}_2\text{CO}_2\text{H}\cdot\text{Cl}^-$ ] was a generous gift from Dr. George Markham (Fox Chase Cancer Center).

**Purification and Assay of Recombinant MSOX.** *Escherichia coli* strain DH1/pMAW was grown at 37 °C in LB media containing carbenicillin as previously described (3). Enzyme purification and routine protein and activity assays were performed as described by Wagner et al. (3). The horseradish peroxidase-coupled assay described by Wagner and Jorns (9) was used to investigate the effect of PCA and other active site ligands on MSOX activity.

**Spectroscopy.** Absorption spectra were recorded using a Perkin-Elmer Lambda 2S spectrometer. All extinction coefficients were determined at pH 8.0. The previously determined extinction coefficient for MSOX at 454 nm ( $\epsilon_{454} = 12\,200\text{ M}^{-1}\text{ cm}^{-1}$ ) (3) was used to calculate a value for the oxidized enzyme at 391 nm ( $\epsilon_{391} = 8940\text{ M}^{-1}\text{ cm}^{-1}$ ). Extinction coefficients for the anionic flavin radical ( $\epsilon_{454} = 3620\text{ M}^{-1}\text{ cm}^{-1}$ ,  $\epsilon_{391} = 24\,900\text{ M}^{-1}\text{ cm}^{-1}$ ) were determined after quantitative conversion of the oxidized enzyme to the radical form by 5-deazariboflavin-mediated photoreduction in the presence of methyl viologen (vide infra). Two-electron reduced MSOX ( $\epsilon_{454} = 948\text{ M}^{-1}\text{ cm}^{-1}$ ,  $\epsilon_{391} = 3120\text{ M}^{-1}\text{ cm}^{-1}$ ) was generated by anaerobic reduction with sarcosine (9).

Spectral titrations with active site ligands were conducted at 25 °C in 50 mM potassium phosphate buffer, pH 8.0. All spectra are corrected for dilution. For comparison of the spectral perturbations observed with different ligands (see Figures 4–7), difference and absolute spectra were normalized to the same initial concentration of uncomplexed MSOX ( $A_{454} = 0.4$ ). (The observed initial  $A_{454}$  varied from about 0.3 to 0.45 in different experiments.) Spectra were also normalized to 100% complex formation to compensate for differences in the maximal extent of complex formation observed in titrations with different ligands. The 100% complex spectra were calculated using the measured complex dissociation constants and spectral data obtained at the highest ligand concentration tested.

**Anaerobic Experiments.** High purity argon (<20 ppm oxygen) containing 1% hydrogen (Scott Medical Gases) was scrubbed to remove traces of oxygen using a Matheson Oxygen Remover (model 64-1008A) followed by passage through a gas washing bottle containing 0.5 mM reduced methyl viologen, 10  $\mu\text{M}$  5-deazariboflavin, 10 mM EDTA, and 0.1 M Tris-HCl, pH 8.0. (Reduced methyl viologen was generated by photoreduction after purging the system with argon.) Anaerobic cuvettes with two sidearms were made anaerobic by bubbling argon through protein-free solutions in the main compartment and aliquots >20  $\mu\text{L}$  in the sidearms. Argon was bubbled over the surface of small aliquots (<20  $\mu\text{L}$ ) of enzymes or other reaction components in the sidearms. Photoreduction experiments were conducted by irradiating the anaerobic sample with two 15-W blue-black fluorescent tubes (Sylvania F15T8BLB).

**Data Analysis.** Data were fit to eqs 1–2 using the curve fit function in Sigma Plot (Jandel Corporation). Equation 1 was used to fit the effect of pH on the absorption spectrum of MSOX.  $Y$  is the observed absorbance at 352 nm at a given pH value.  $A$  and  $B$  are the calculated absorbance at 352 nm at low and high pH values, respectively. Equation 2 was used for analysis of spectrophotometric titration data for complex formation between MSOX and various ligands.  $Y$  and  $A$  are the observed and maximal absorbance change at the wavelength selected for analysis, respectively,  $X$  is the concentration of the varied ligand, and  $K$  is the complex dissociation complex.

$$Y = \frac{AH^+ + BK_a}{H^+ + K_a} \quad (1)$$

$$Y = \frac{AX}{X + K} \quad (2)$$

**Crystallization and Data Collection.** Crystals of MSOX were grown by the sitting drop method as described previously (7). Equal volumes of 5  $\mu$ L each of protein solution (7 mg/mL in 20 mM Tris-HCL, pH 8.0) and reservoir solution (2.1 M sodium/potassium phosphate buffer, pH 7.0) were mixed and allowed to equilibrate. Single crystals of MSOX were soaked in the presence of one of the three active site ligands DMG, MSEA, or MTEA as indicated in Table 5. Soaking times ranged from 15 min to 15 h at concentrations of 9–50 mM.

X-ray data were recorded from single crystals at 100 °K on a Rigaku R-axis IV image plate detector using a Ni-filtered, mirror-focused X-ray beam obtained from a Rigaku RU200 X-ray generator operated at 5 keV power. One crystal was used for each data set with the exception of MTEA in which partial data sets from two crystals (114 frames from the first and 42 frames from the second) were combined. The crystals were monoclinic, space group  $P2_1$ , and all isomorphous to each other; the unit cell parameters are  $a = 72.6$  Å,  $b = 69.5$  Å,  $c = 73.5$  Å, and  $\beta = 94.1^\circ$ , and there are two molecules per asymmetric unit. Spot integration and data scaling were carried out using HKL (10). The data were generally 88–98% complete and scaled to the outer resolution limits (1.9–1.8 Å) with  $R_{\text{merge}}^2$  between 0.057 and 0.095. The data collection statistics are summarized in Table 5.

Structure refinement and electron density map calculations were carried out using CNS (11), and 10% of the reflections were selected randomly and set aside as a test set for cross validation (12). Reflections from infinity to 1.9- or 1.8-Å resolution for each data set were included in the refinements, and a bulk solvent correction was applied (13). Coordinates for the ligands bound at the active site were obtained from the Cambridge Structure Database (14). Noncrystallographic symmetry (NCS) restraints were applied to the two protein molecules in the asymmetric unit during refinement (with NCS weights set to 300 for both main and side chain atoms), and reflections with  $\sigma(I) < 0.0$  were omitted; the differences between B-factors for bonded atoms were restrained with target standard deviations of 1.5 Å<sup>2</sup> for main chain and 2.0 Å<sup>2</sup> for side chain atoms. Model building and analysis of the structure were carried out on a Silicon Graphics workstation using Turbo-Frodo (15). From one to three side chains and, in two of the complexes, the ligand in each molecule were modeled in two alternate conformations among the complexes. In addition, during the final stages of refinement, two short polypeptide segments plus two side chains, all near the protein surface, consistently differed from each other in the two subunits, and the NCS restraints were removed from these residues.

## RESULTS

**MSOX Stability.** MSOX is extremely stable at slightly alkaline pH, but a sharp decrease in stability is observed at pH < 7. At pH 8, MSOX is stable upon prolonged incubation at room temperature. At pH 7, the enzyme retains 90% of its activity after 24 h at 4 °C. Almost no activity is detectable after a similar incubation at pH 6.0.

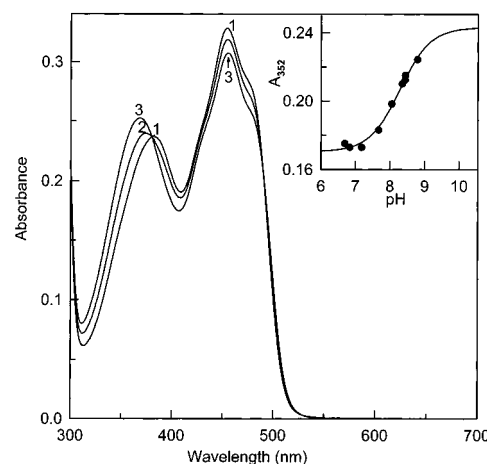


FIGURE 1: Effect of pH on the absorption spectrum of MSOX. Curves 1–3 were recorded at 4 °C in 50 mM potassium phosphate buffer at pH 7.18, 8.05, and 8.79, respectively. The inset shows a plot of MSOX absorbance at 352 nm as a function of pH. The curve shows a fit of the data points (solid circles) to a theoretical pH titration curve.

**pH Dependence of the Absorption Spectrum.** The absorption spectrum of MSOX in the oxidized state is markedly dependent on pH. At pH 7.18, MSOX exhibits absorption maxima at 454 and 381 nm. As the pH is increased from 7.18 to 8.79, the 381 nm peak undergoes an increase in absorbance and a pronounced hypsochromic shift to 368 nm, whereas a decrease in absorbance is observed at 454 nm (Figure 1). The spectral changes are very similar to that observed with free oxidized FAD upon ionization at the N(3)H position ( $pK_a = 10.4$ ) (16). Analysis of MSOX absorbance changes at 352 nm as a function of pH yields a  $pK_a$  value of 8.28, a downward shift of more than two pH units as compared with free flavin.

**Photoreduction of MSOX.** MSOX can be photoreduced at pH 8.0 under anaerobic conditions through mediation by 5-deazariboflavin (17) to form a red, anionic radical. Radical formation is indicated by the development of an intense new absorption band at 391 nm, accompanied by the bleaching of the 454-nm band of the oxidized enzyme (Figure 2). Similar results are obtained when the reaction is conducted at pH 7.0.<sup>3</sup> Radical formation is fairly rapid (~10 min) and fully reversible upon aeration. Transfer of a second electron to form the fully reduced enzyme is extremely slow (26 h, data not shown). This prolonged illumination resulted in ~50% cleavage of the covalent flavin linkage, as judged by microfiltration of the reoxidized enzyme. Inclusion of methyl viologen (25  $\mu$ M) as an electron carrier resulted in a dramatic decrease in the time required for the second electron transfer (3 min versus 26 h), which was now fully reversible upon aeration. A similar effect has been observed with methyl viologen and lactate oxidase. It has been suggested that the positive charge of one-electron reduced methyl viologen helps to overcome an apparent kinetic barrier in the reduction of negatively charged flavin radicals (18).

**Stability of the Flavin Radical.** The MSOX radical formed in the presence of methyl viologen at pH 8.0 was stable in the dark and did not disproportionate to a mixture of fully oxidized and two-electron reduced flavin even after pro-

<sup>2</sup> The definitions of  $R_{\text{merge}}$ ,  $R$ , and  $R_{\text{free}}$  are given in the legend to Table 5.

<sup>3</sup> P. Khanna and M. S. Jorns, unpublished results.



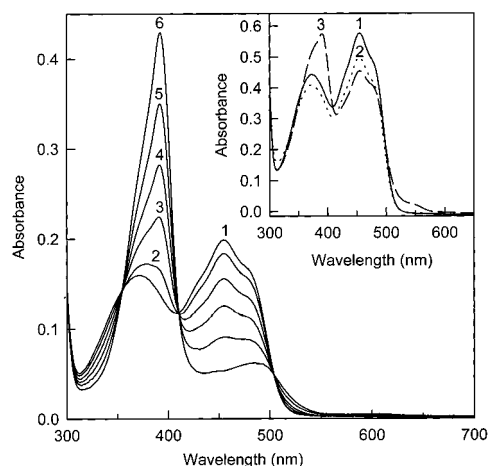


FIGURE 2: Formation of the Anionic Radical. Curve 1 shows the absorption spectrum of the oxidized enzyme ( $16.3 \mu\text{M}$ ) in 10 mM potassium phosphate buffer, pH 8.0, containing 8 mM EDTA and  $0.25 \mu\text{M}$  5-deazariboflavin. Curves 2–6 were recorded after illumination at room temperature for 10, 30, 60, 90, and 585 s, respectively. Inset: Curve 1 (solid line) is the absorption spectrum of the oxidized enzyme ( $46 \mu\text{M}$ ) in 50 mM potassium phosphate, pH 8.0, containing  $16.6 \mu\text{M}$  methyl viologen under anaerobic conditions. Curve 2 (dotted line) was recorded after adding  $37 \mu\text{M}$  sarcosine, which generated  $5.6 \mu\text{M}$  two-electron reduced enzyme, owing to residual oxygen in the cuvette. Curve 3 (dashed line) was recorded after a 3-week incubation of the sample at room temperature. The spectrum obtained after admitting air superimposed with curve 1.

longed storage (87 h), suggesting that thermodynamic, rather than kinetic, factors could account for the observed radical stability. In a separate experiment, a mixture of fully oxidized ( $40.4 \mu\text{M}$ ) and two-electron reduced ( $5.6 \mu\text{M}$ ) MSOX was prepared by anaerobic reduction with a limited amount of sarcosine and then allowed to incubate in the dark in the presence of methyl viologen as electron carrier. A significant amount of radical formation was observed after a 3-week incubation, as judged by the development of a new absorption band at 391 nm (Figure 2, inset). The extinction coefficients of the oxidized, radical, and two-electron reduced forms of MSOX at 454 and 391 nm were used to calculate the concentration of the various redox species in the incubated sample (35.2, 10.4, and  $0.4 \mu\text{M}$ , respectively). The estimated radical content ( $10.4 \mu\text{M}$ ) is close to the upper limit ( $11.2 \mu\text{M}$ ) expected if the redox equilibrium lies strongly in favor of radical formation.

**Sulfite Complex.** MSOX forms a covalent flavin·sulfite complex, similar to that observed with other flavoprotein oxidases (19), as judged by the characteristic, isosbestic bleaching of the oxidized flavin absorption spectrum upon reaction with sulfite at pH 7 (data not shown). However, complex stability could not be evaluated because complex formation was extremely slow ( $t_{1/2} = 27$  h with 100 mM sulfite at  $4^\circ\text{C}$ ), and the reactions could not be followed to completion owing to enzyme denaturation.

**Identification of Active Site Ligands.** Compounds that bound to the MSOX active site were identified based on their ability to perturb the flavin absorption spectrum, as illustrated by titration data obtained with methoxyacetate (Figure 3). The wavelength of maximal absorbance change (497 nm) was determined from difference spectra recorded during the titration (Figure 3A). The complex dissociation constant ( $K_d = 28.2$  mM) was determined by fitting absorbance

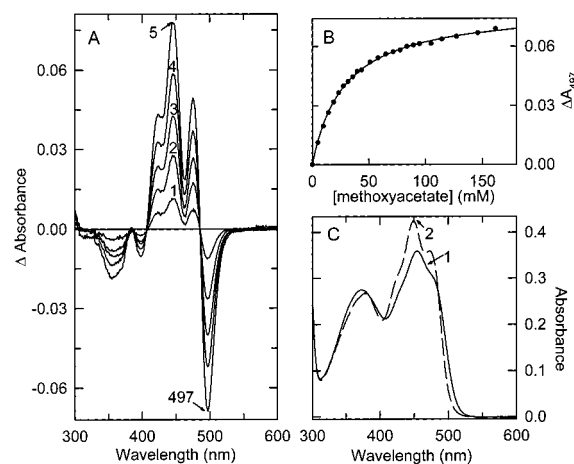


FIGURE 3: Titration of MSOX with methoxyacetate. Panel A: Curves 1–5 are difference spectra recorded after adding 4.93, 14.4, 27.6, 51.2, and 162 mM methoxyacetate, respectively, to  $29.4 \mu\text{M}$  MSOX. Panel B: The observed decrease in absorbance at 497 nm (solid circles) is plotted as a function of the methoxyacetate concentration. The solid line is a fit of the data to a theoretical binding curve ( $K_d = 28.2$  mM). Panel C: Curves 1 and 2 are absolute spectra recorded after adding 0 and 162 mM methoxyacetate, respectively. The latter spectrum represents 85.1% complex formation, as estimated based on the observed  $K_d$  value.



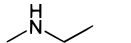
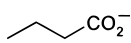
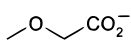
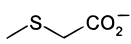
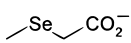
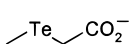




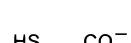
changes at 497 nm to a theoretical binding curve (Figure 3B). Absolute spectra show that methoxyacetate mainly effects the 454-nm band of free MSOX, which undergoes a 5-nm hypsochromic shift accompanied by an increase in extinction and the appearance of a pronounced shoulder at 473 nm (Figure 3C).

Each active site ligand identified in these studies (see Tables 1 and 2) caused a unique spectral change and acted as an enzyme inhibitor. Steady-state kinetic studies with pyrrole-2-carboxylate showed that the compound acted as a competitive inhibitor with respect to sarcosine. The observed inhibition constant ( $K_i = 1.21$  mM) is in good agreement with the complex dissociation constant as determined by spectral titration ( $K_d = 1.37$  mM).

**Substrate Binding Determinants.** The substrate carboxylate group is essential for binding, since simple amines, like ethylmethylamine, do not perturb the MSOX absorption spectrum or inhibit MSOX activity. The amino group of sarcosine is not essential, as judged by results obtained with a series of analogues ( $\text{CH}_3\text{XCH}_2\text{CO}_2^-$ ) in which the substrate amino group is replaced by  $\text{CH}_2$ , O, S, Se, or Te. A progressive increase in binding affinity is observed within this series (Table 1). The observed dissociation constant when  $\text{X} = \text{Te}$  is only about 2-fold larger than the value estimated for sarcosine from steady-state kinetic data (9).

The methyl group of sarcosine is also not essential since binding is observed when the methyl group in  $\text{CH}_3\text{XCH}_2\text{CO}_2^-$  ( $\text{X} = \text{NH}$ , O, S) is replaced by hydrogen (Table 1). The methyl group does, however, contribute to binding energy since the unmethylated derivatives are bound more weakly. The methyl group contribution to binding energy varied from  $-3.79$  to  $-0.65$  kcal/mol, depending on the nature of the heteroatom ( $\text{N} > \text{O} > \text{S}$ ) (Table 3). The contribution of the methyl group to the observed spectral perturbation also varied, depending on the nature of X. Loss of the methyl group has little effect when  $\text{X} = \text{O}$ , as judged by the similar difference spectra observed with methoxyacetate and gly-

Table 1: Sarcosine Analogs as MSOX Ligands

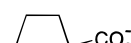
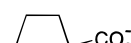
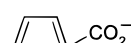
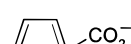

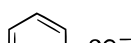
compound		$K_d$ (mM)	CT Complex	
			Formed	$\lambda_{max}$
sarcosine		0.6 <sup>1</sup>	ND	-
ethylmethanamine		NOT BOUND	-	-
butyrate		118	NO	-
methoxyacetate		28.2	NO	-
methylthioacetate		2.60	YES	532
methylselenoacetate		2.13	YES	585
methyltelluroacetate		1.46	YES	696
dimethylglycine		17.4	NO	-
dimethylthioacetate		20.5	NO	-
glycine		359	NO	-
glycolate		183	NO	-
thioglycolate		7.72	YES	508

<sup>1</sup> Estimated from steady-state kinetic data (9). All other values were determined in this study by spectral titration.

colate (Figure 4A). A significant difference is observed with methylthioacetate versus thioglycolate ( $X = S$ ). Both compounds form charge-transfer complexes with MSOX, as judged by the development of a new absorption band in the long wavelength region (Figure 4B). Loss of the methyl group, however, results in a 24-nm hypsochromic shift in the position of the charge-transfer band from 532 to 508 nm (Figure 4B). The spectral contribution of the methyl group when  $X = NH$  is unknown since data could be obtained only for the glycine complex (Figure 4A, curve 3).

**Does MSOX Bind the Zwitterionic or the Anionic Form of Sarcosine?** Although the anionic form of sarcosine is likely to be the species that undergoes oxidation during the MSOX reaction, the zwitterionic form will predominate in solution at neutral pH. Studies with the methionine repressor protein show that compounds containing a protonated amino group and the corresponding sulfonium derivatives are good structural analogues (20). Dimethylthioacetate  $[(CH_3)_2S^+CH_2CO_2^-]$  should, therefore, be a good analogue for the zwitterionic  $[(CH_3)_2NH^+CH_2CO_2^-]$  but not the anionic  $[(CH_3)_2NCH_2CO_2^-]$  form of dimethylglycine. MSOX forms very similar complexes with dimethylglycine and dimethylthioacetate, as

Table 2: Aromatic Analogs as MSOX Ligands

compound		$K_d$ <sup>1</sup> (mM)	CT Complex	
			Formed	$\lambda_{max}$
L-proline		260 <sup>2</sup>	ND <sup>3</sup>	-
pyrrole-2-carboxylate		1.37	YES	608
2-furoate		29.0	YES	502
thiophene-2-carboxylate		20.2	YES	486
benzoate		61.5	NO	-

<sup>1</sup>  $K_d$  values were determined in this study by spectral titration at 25 °C, unless otherwise noted. <sup>2</sup>  $K_d$  estimated from reductive half-reaction kinetic data at 4 °C (9). <sup>3</sup> ND, not determined.

Table 3: Contribution of the Methyl Group to the Stability of MSOX•RXCH<sub>2</sub>CO<sub>2</sub><sup>-</sup> Complexes

compound	compound		$\Delta G_a$ (kcal/mol)	$\Delta\Delta G_a$ (CH <sub>3</sub> group) (kcal/mol)
	R	X		
sarcosine <sup>a</sup>	CH <sub>3</sub>	H <sub>2</sub> N <sup>+</sup>	-4.40 <sup>b</sup>	-3.79
glycine <sup>a</sup>	H	H <sub>3</sub> N <sup>+</sup>	-0.61	0
methoxyacetate	CH <sub>3</sub>	O	-2.11	-1.10
glycolate	H	O	-1.01	0
methylthioacetate	CH <sub>3</sub>	S	-3.53	-0.65
thioglycolate	H	S	-2.88	0

<sup>a</sup> The structure of X is shown for the zwitterionic form. <sup>b</sup> Estimated from steady-state kinetic data (9). All other values were determined in this study by spectral titration.

judged by the observed spectral perturbations (Figure 5) and complex dissociation constants ( $K_d = 17.4$  and 20.5 mM, respectively). The results indicate that MSOX binds the zwitterionic form of dimethylglycine, suggesting a similar binding mode for sarcosine. This conclusion is supported by the structural data obtained for the MSOX•dimethylglycine complex, as will be described below.

**Complexes with Aromatic Carboxylates.** Although L-proline is a poor substrate (9), aromatic heterocyclic carboxylates containing a five-membered ring and various heteroatoms ( $X = NH, O, S$ ) are reasonably good ligands for MSOX (Table 2). The complex formed with pyrrole-2-carboxylate ( $\Delta G_a = -3.91$  kcal/mol) is approximately 1.7 kcal/mol more stable as compared with complexes where the heteroatom is sulfur or oxygen ( $\Delta G_a = -2.31$  or  $-2.10$  kcal/mol, respectively). This difference is attributed to hydrogen bond formation between NH in pyrrole-2-carboxylate and the backbone carbonyl of Gly344 (7), an interaction not possible when  $X = S$  or O. Benzoate is bound 2- to 45-fold less strongly than the heterocyclic carboxylates.

**Charge-Transfer Complexes.** Charge-transfer complexes are formed with MSOX and  $CH_3XCH_2CO_2^-$  when  $X = S, Se, \text{ or } Te$ , as evidenced by the appearance of a new intense absorption band at longer wavelengths (Figure 6). The energy

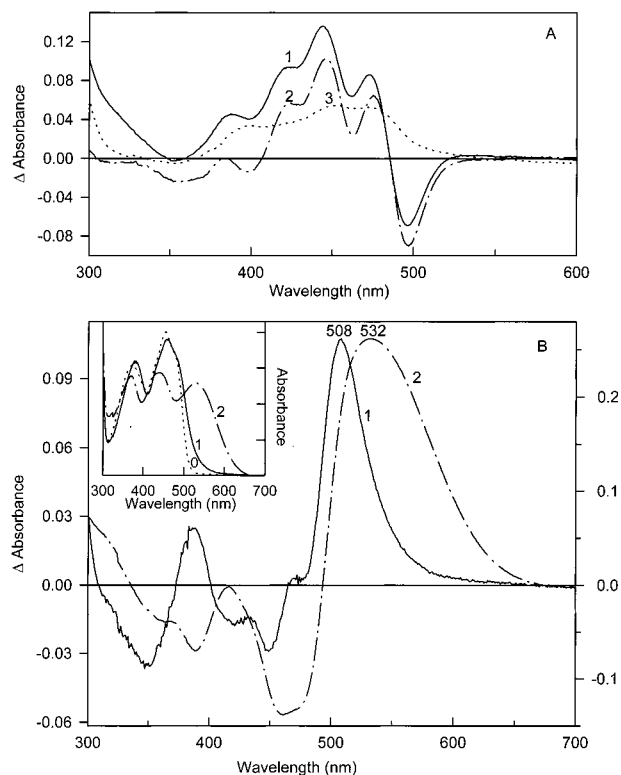


FIGURE 4: Comparison of the spectral perturbations observed for MSOX complexes formed with  $RXCH_2CO_2^-$  when  $R = CH_3$  or  $H$  and  $X = O, NH,$  or  $S$ . Difference and absolute spectra were normalized to the same initial concentration of uncomplexed MSOX ( $A_{454} = 0.4, 32.8 \mu M$  MSOX) and to 100% complex formation, as described in Experimental Procedures. Panel A shows difference spectra obtained for the complexes formed with glycolate (curve 1, solid line) and methoxyacetate (curve 2, dot-dashed line). Curve 3 (dotted line) is the difference spectrum obtained for the glycine complex. Panel B compares difference and absolute (inset) spectra observed for MSOX complexes formed with thioglycolate (curve 1, solid line) and methylthioacetate (curve 2, dot-dashed line). Difference spectra for thioglycolate and methylthioacetate are plotted using the  $\Delta$  absorbance scales shown on the left and right, respectively. The absolute spectrum of uncomplexed MSOX is shown by curve 0 (dotted line) in the inset.

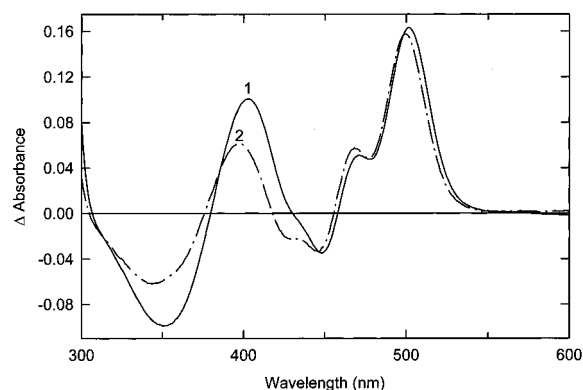


FIGURE 5: Comparison of difference spectra obtained for complexes formed with MSOX and dimethylthioacetate (curve 1, solid line) or dimethylglycine (curve 2, dot-dashed line). Spectra were normalized as described in the legend to Figure 4.

of the charge-transfer bands varied, depending on the nature of  $X$  ( $S > Se > Te$ ), as judged by the long wavelength absorption maxima of the complexes (532, 585, and 696 nm, respectively). As will be described, the structures of the complexes when  $X = Se$  or  $Te$  have been determined and

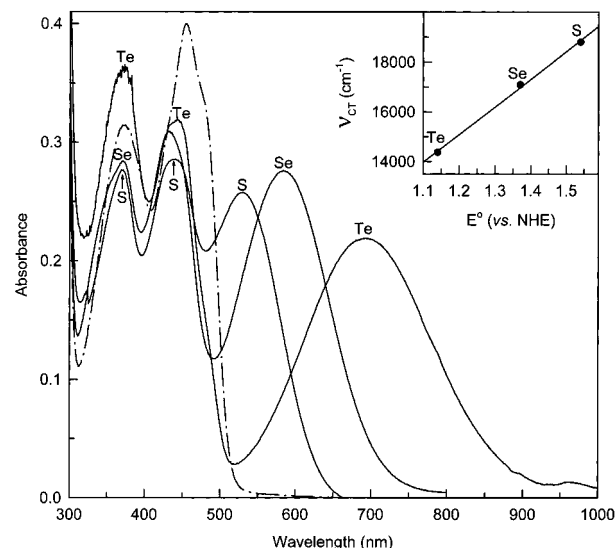


FIGURE 6: Charge-transfer complexes formed with MSOX and  $CH_3XCH_2CO_2^-$ . The absorption spectrum of free MSOX (dot-dashed line) is compared with the complexes (solid lines) formed when  $X = S, Se,$  or  $Te$ . All spectra are normalized as described in the legend to Figure 4. The inset shows a plot of the energy of the charge-transfer bands versus  $E^0$  values of the ligands, estimated as described in the text.

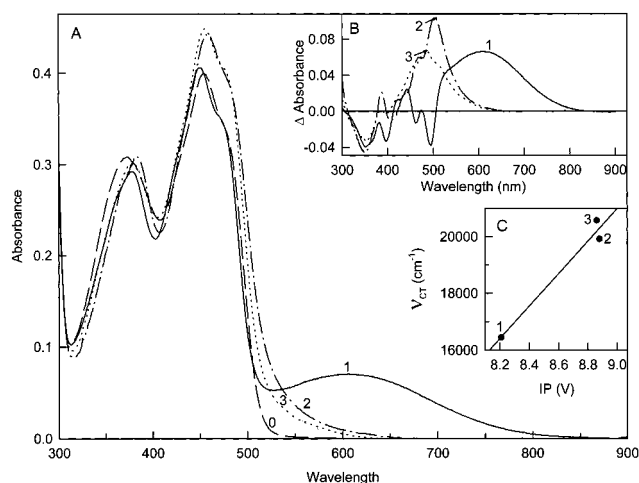


FIGURE 7: Charge-transfer complexes formed with MSOX and heterocyclic carboxylates. Panel A: Absorption spectrum of free MSOX (curve 0, dashed line) is compared with the complexes formed with pyrrole-2-carboxylate (curve 1, solid line), 2-furoate (curve 2, dot-dashed line), and thiophene-2-carboxylate (curve 3, dotted line). The corresponding difference spectra are shown in panel B. All spectra are normalized as described in the legend to Figure 4. Panel C shows a plot of the energy of the charge-transfer bands versus the IP values of the ligands, as described in the text.

exhibit certain differences as compared the structure previously determined for methylthioacetate ( $X = S$ ) (7). Charge-transfer complexes are also formed with MSOX and aromatic carboxylates containing a heterocyclic five-membered ring (Figure 7A). The charge-transfer bands when  $X = O$  or  $S$  are not well-resolved in the absolute spectra owing to overlap with the high wavelength edge of the flavin absorption spectrum. These band positions were estimated from difference spectra (Figure 7B). The energy of the charge-transfer bands with heterocyclic carboxylates varied depending on the nature of the heteroatom ( $S > O \gg NH$ ) ( $\lambda_{max} = 486, 502,$  and  $608$  nm, respectively).

Table 4: Association Energies for MSOX·XCH<sub>2</sub>CO<sub>2</sub><sup>−</sup> Complexes versus Flavin-Receptor·X Complexes

X	MSOX complex <sup>a</sup>		model complex <sup>b</sup>	
	$\Delta G_a$ (kcal/mol)	$\Delta\Delta G_a$ (donor- $\pi$ ) (kcal/mol)	$\Delta G_a$ (kcal/mol)	$\Delta\Delta G_a$ (donor- $\pi$ ) (kcal/mol)
CH <sub>3</sub> CH <sub>2</sub> -	-1.27	0	-4.04	0
CH <sub>3</sub> -O-	-2.11	-0.84	-4.53	-0.49
CH <sub>3</sub> -S-	-3.53	-2.26	-4.99	-0.95
CH <sub>3</sub> -Se-	-3.64	-2.37	ND <sup>b</sup>	
CH <sub>3</sub> -Te-	-3.87	-2.60	ND	

<sup>a</sup> 25 °C, aqueous, pH 8. <sup>b</sup> 23 °C, CDCl<sub>3</sub> (39). <sup>c</sup> ND, not determined.

**Refinement of MSOX·Inhibitor Complex Structures.** The structures of the MSOX·inhibitor complexes with methyl-selenoacetate (MSEA), methyltelluroacetate (MTEA), and dimethylglycine (DMG) were refined directly, starting with the coordinates of an isomorphous complex of MSOX with 2-furoate, which was determined at 1.3 Å resolution,<sup>4</sup> but with all ligands, solvent molecules, and alternate conformers omitted. For consistency in structural comparisons, the structures of the MTA and PCA complexes with MSOX<sup>5</sup> (7) were also refined in the same way using CNS and starting with the bare 2-furoate complex. Several cycles of positional and temperature factor refinement, followed by interactive model building and automatic solvent placement with manual examination, were carried out. This procedure utilized electron density difference maps calculated with Fourier coefficients (2*Fo*-*Fc*) and (*Fo*-*Fc*), where *Fo* and *Fc* are the observed and calculated structure factors, respectively. During refinement, it was discovered that both MSEA and MTEA were each bound to MSOX in two alternate confor-

mations that differ only in the placement of the selenium and tellurium atoms (see below). In addition, a peak having strong density in (*Fo*-*Fc*) difference maps was located 2.95 Å from the S<sup>γ</sup> of Cys262 in each monomer. This peak was modeled as Te<sup>−</sup>, and its occupancy refined to a value of 0.22, while its temperature factor was fixed to the average value of the protein; its presence may have resulted from partial degradation of the MTEA inhibitor in one of the MTEA-soaked crystals, probably the second, which represented 28% of the data.

The quality of the refined structures and the resulting electron density maps of all three enzyme·ligand complexes of MSOX is high (Table 5, Figures 8A, 9A). The three new enzyme·inhibitor complexes (with MTEA, MSEA, and DMG) are all in the “closed” conformation, like the MTA and PCA complexes described previously (7), with the flavin ring and ligands shielded from solvent. The *R*<sup>2</sup> and *R*<sub>free</sub><sup>2</sup> range from 0.167 to 0.193 and 0.221 to 0.231, respectively, with RMSD in bond lengths and angles of 0.008–0.013 Å and 1.56–1.76°, respectively. Between 606 and 800 water molecules are included in the structures, and each protein molecule contains one bound chloride ion. The Ramachandran plot (21, 22) for each crystal structure shows that only one residue lies in a sterically disallowed region in each molecule of the asymmetric unit, Asp47. This residue, which is located in a coil between the flavin binding and catalytic domains and whose side chain is oriented differently in the two NCS-related molecules, is found in the same configuration in the structures of free MSOX and its complexes with MTA and PCA (7). The final refinement statistics are shown in Table 5.

Table 5: Data Collection and Structure Determination of MSOX·Ligand Complexes

	DMG	MSEA	MTEA	MTA <sup>a</sup>	PCA <sup>a</sup>
reagent (conc, time)	50 mM, 15 h	9 mM, 30'	25 mM, 15'		
resolution (Å)	∞–1.8	∞–1.9	∞–1.9	∞–2.0	∞–2.1
data collection					
no. of reflections	60143	56287	65450		
completeness (all/outer 0.05 Å shell, %)	88.3/36.7	97.9/97.5	94.2/62.3		
<i>R</i> <sub>merge</sub> <sup>b</sup> (all/outer)	0.057/0.333	0.095/0.336	0.091/0.248		
<i>I</i> / <i>σ</i> <sup>c</sup> (all/outer)	26.3/3.8	15.9/3.0	17.7/4.5		
redundancy (all/outer 0.05 Å shell)	4.3/2.8	3.0/2.8	2.8/2.1		
refinement					
<i>R</i> <sub>cryst</sub> <sup>d</sup> (all/outer 0.05 Å shell)	0.167/0.288	0.193/0.336	0.175/0.297	0.179/0.278	0.165/0.184
<i>R</i> <sub>free</sub> <sup>e</sup> (all/outer 0.05 Å shell)	0.211/0.356	0.231/0.394	0.214/0.331	0.219/0.311	0.215/0.240
no. protein atoms (non-H) <sup>f</sup>	6018	6018	6018	6018	6018
<i>B</i> (Å <sup>2</sup> )	20.2	29.4	19.9	21.9	25.3
no. of alternate conformers	4	8	8	2	2
no. FAD atoms (non-H) <sup>f</sup>	106	106	106	106	106
<i>B</i> (Å <sup>2</sup> )	14.8	24.9	14.9	15.4	18.6
no. of chloride ions <sup>f,g</sup>	2	2	2	2	2
<i>B</i> (Å <sup>2</sup> )	17.2	24.7	19.9	17.6	19.1
no. of ligand atoms (non-H) <sup>f</sup>	14	14	16	12	16
<i>B</i> (Å <sup>2</sup> )	19.2	28.6	21.6	25.5	25.3
no. of solvent molecules <sup>f</sup>	784	606	800	549	624
<i>B</i> (Å <sup>2</sup> )	33.4	37.2	32.1	31.5	35.6
RMSD					
bonds (Å)	0.013	0.011	0.008	0.009	0.010
angles (°)	1.76	1.67	1.56	1.62	1.63
$\Delta B$ (main-main, Å <sup>2</sup> )	1.6	1.4	2.0	1.2	2.0
$\Delta B$ (main-side, Å <sup>2</sup> )	2.0	1.6	2.3	1.6	2.2
$\Delta B$ (side-side, Å <sup>2</sup> )	2.8	2.3	3.0	2.4	3.2

<sup>a</sup> Data for PCA and MTA were recorded as described previously in Trickey et. al, 1999 (7). <sup>b</sup>  $R_{\text{merge}} = \sum_i \sum_h |I_i(h) - I_i(h)| / \sum_i \sum_h I_i(h)$ , where *I*<sub>i</sub>(*h*) and *I*(*h*) are the *i*th and mean measurements of reflection *h*. <sup>c</sup> *I*/*σ*(*I*) is the average signal-to-noise ratio for merged reflection intensities. <sup>d</sup>  $R = \sum_h |F_o - F_c| / \sum_h |F_o|$ , where *Fo* and *Fc* are the observed and calculated structure factor amplitudes of reflection *h*. <sup>e</sup> *R*<sub>free</sub> is the test reflection data set, about 10% selected randomly for cross validation during crystallographic refinement (12). <sup>f</sup> Per asymmetric unit, which contains two molecules of MSOX.



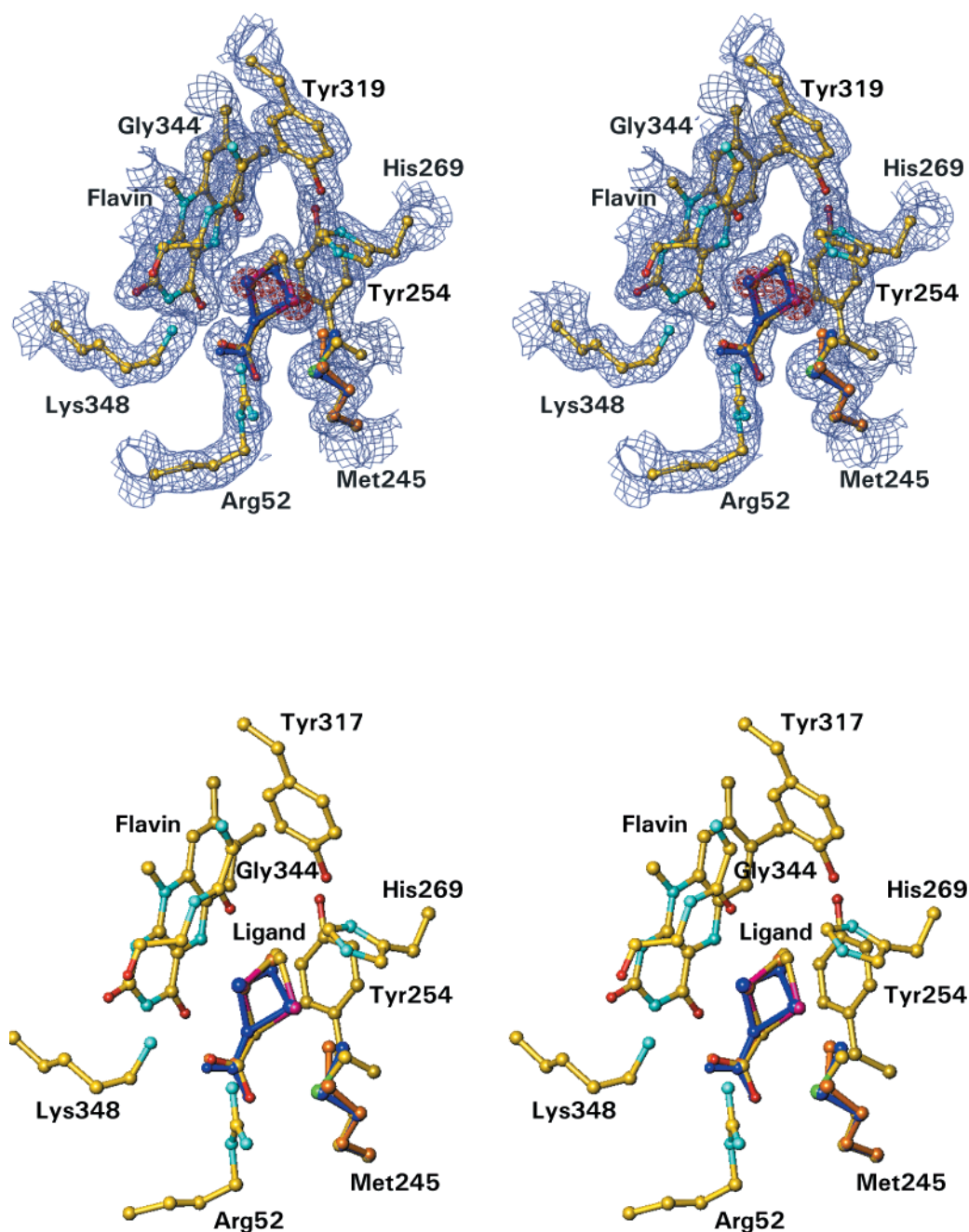


FIGURE 8: Binding of MTEA, MSEA, and MTA to the active site of MSOX. (A) Stereoview of the electron density for MSOX·MTEA complex. Ball-and-stick representation of surrounding side chains are shown in atom colors with carbon in yellow, nitrogen in azul, oxygen in red, sulfur in green, and Te in violet. Ligands MSEA (dark blue) and MTA (gold) are also included. The MTA structure is difficult to see since it virtually superimposes with the MTEA and MSEA structures. Both the Te and the Se atoms are present in two alternate conformations, as indicated in the electron density for Te. Contours are drawn at 1.25  $\sigma$  (blue) and 7  $\sigma$  (red). The side chains of Met245 are also shown for MSEA (dark blue) and MTA (gold) to indicate the successive displacement of its C $\epsilon$  atom by the alternate conformers of Se and Te, respectively. (B) Same as panel A but with the electron density omitted for clarity.

*Structure of MSOX Complexes with Methylselenoacetate (MSEA) and Methyltelluroacetate (MTEA).* MSEA and MTEA bind to MSOX in two discrete conformations (Figure 8). In one conformation, the four coplanar atoms C1–C2–X3–C4 (X = Se, Te) lie nearly parallel to the flavin ring and effectively superimpose on the MTA structure (where

X = S; Figure 8B) (7). The carboxylate group is about 20° out of the plane of the other four atoms. One carboxylate oxygen is hydrogen bonded to N $\epsilon$  of Arg52; the other is hydrogen bonded to N $\epsilon^2$  of Arg52 and to N $\epsilon$  of Lys348. The heavy atoms (S, Se, and Te) are located about 3.3 Å above the flavin and equidistant from the closest ring atoms C(4) and C(4a). In the alternate conformation exhibited by MSEA and MTEA, the plane of C2–X3–C4 is rotated about 70° out of the plane defined by the first conformer through movement of atom X3 only, with the remaining atoms of the ligands maintaining essentially the same positions. The

<sup>4</sup> P. Trickey, Z.-w. Chen, M. S. Jorns, and F. S. Mathews, unpublished results.

<sup>5</sup> The structure of the MTA complex with MSOX utilized a crystal of selenomethionine-substituted MSOX, which is catalytically very similar to native MSOX.



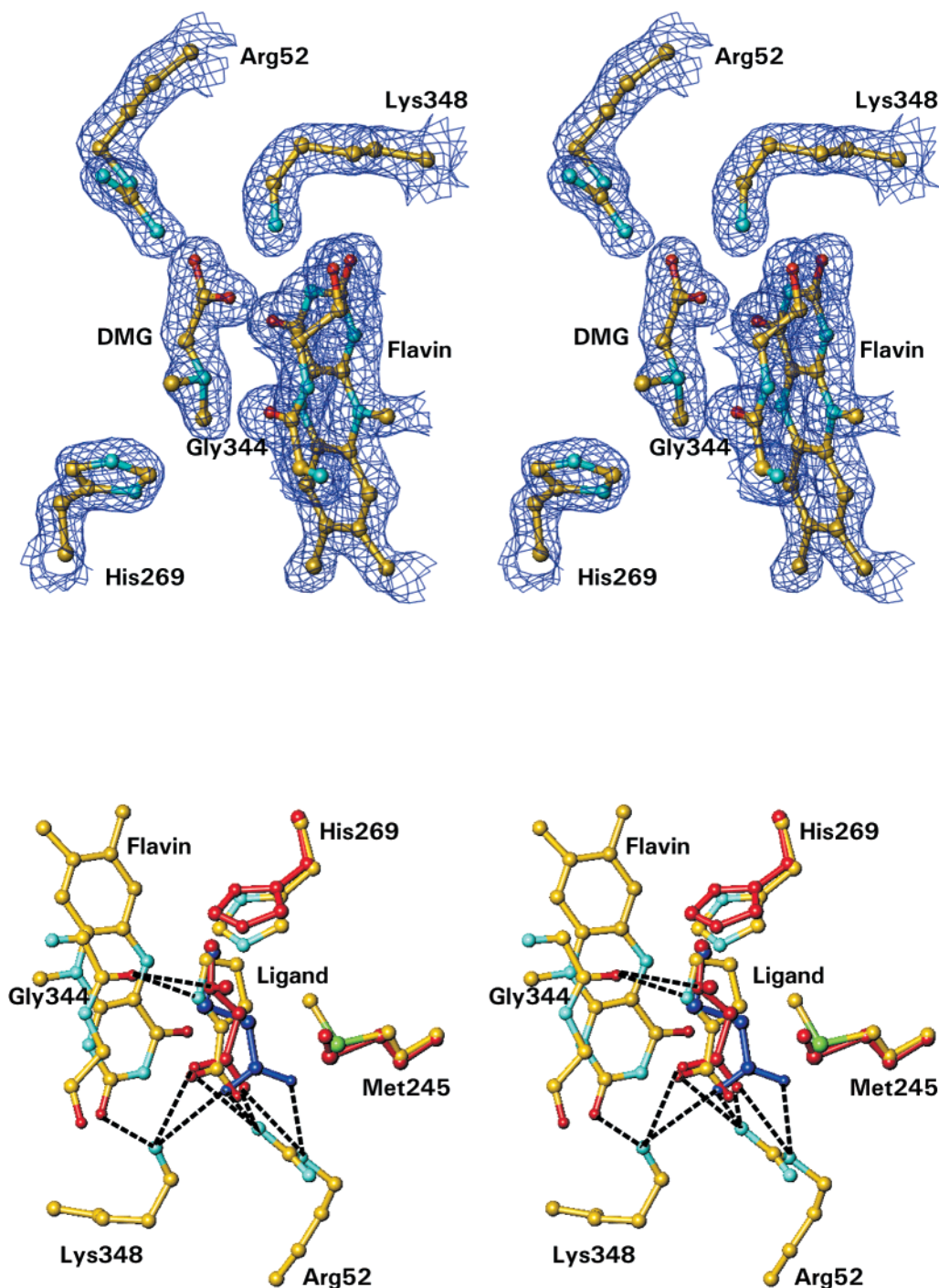


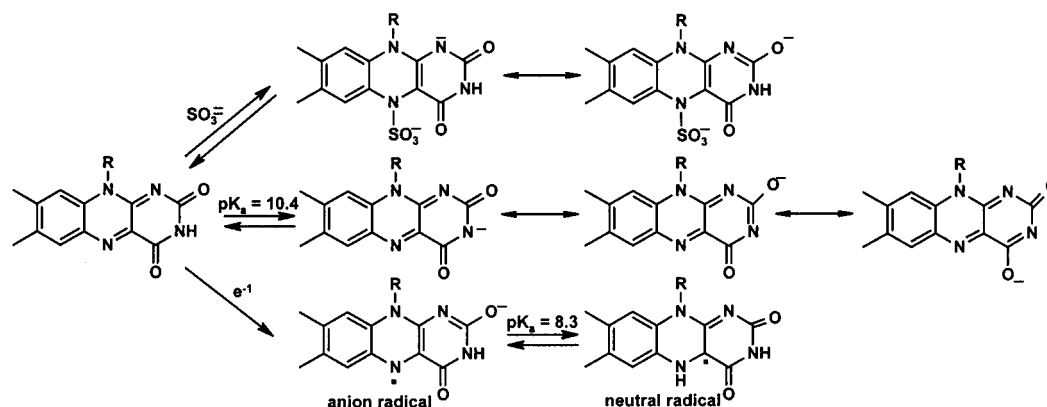
FIGURE 9: Binding of dimethylglycine in the active site of MSOX. (A) Stereoview of the  $2F_o - F_c$  electron density difference map of the MSOX·DMG complex in the active site. A ball-and-stick representation for DMG, the flavin ring, several interacting side and main chain atoms are included. The contour level is  $1.5 \sigma$ . The atom colors are carbon (yellow), nitrogen (azur), oxygen (red), and sulfur (green). (B) Comparison of the binding of DMG (red), MTA (dark blue), and PCA (atom colors, see caption to Figure 8A) in the MSOX active site. Hydrogen bonding of the ligands to nearby side chains are indicated by dashed lines. Since the carboxylates of DMG and PCA almost superimpose, only one dashed line is shown for both sets of atoms. The side chains of Met245 and His 269 that are displaced by DMG are also shown in red.

separation of the two alternate positions for Se and Te is about  $2.0 \text{ \AA}$ . The only structural change that takes place within the protein is a movement of atom C $^\epsilon$  of Met245 that occurs in response to the binding of the Se and Te atoms in their alternate positions. The  $X_3$  torsion angle changes by about  $-50$  and  $-75^\circ$ , respectively, so that the Met C $^\epsilon$ –Se and Met C $^\epsilon$ –Te distance is  $3.1$  and  $3.4 \text{ \AA}$ , respectively. The occupancies of the alternate Se and Te sites were set to  $0.35$

and  $0.5$ , respectively, with the result that their temperature factors were consistent with the rest of the structures.

*Structure of the MSOX Complex with Dimethylglycine (DMG).* The orientation of DMG is clearly defined in the electron density (Figure 9A). DMG is bound to MSOX at three points in a manner very similar to the binding of PCA. The two carboxylate oxygen atoms interact with Arg52 and Lys348, with one oxygen atom hydrogen bonded to NE of

Scheme 1: Anionic Flavin Ring Forms



Arg52 and the other to Arg52 NH<sub>2</sub> and Lys348 NZ (Figure 9B). The DMG carboxylate interactions are very similar to those observed for PCA; significantly different interactions are observed for the carboxylates in MTA, MSEA, and MTEA that are differently positioned. The dimethylammonium moiety of DMG is slightly tilted upward, away from the flavin ring, so that the nitrogen atom (3.8 Å above the flavin ring) is able to form a hydrogen bond to the carbonyl oxygen of Gly344. DMG appears to be in the neutral zwitterionic form, with its nitrogen atom protonated and its carboxylate group deprotonated, with Gly344 O serving as a hydrogen bond acceptor and the side chains of Arg52 and Lys348 serving as hydrogen bond donors, respectively. One of the methyl groups of DMG is positioned very close to the binding site of C4 of MTA and is in van der Waals contact with the hydroxyl of Tyr317, the plane of Tyr254 and the carbonyl oxygen of Gly344. The other methyl group is in van der Waals contact with atoms C<sup>ε1</sup> and N<sup>δ1</sup> of His269. To accommodate the close approach of the methyl group, the side chain of His269 is tilted upward, away from the methyl group, by about 15° as compared to the MSOX•MTA complex (Figure 9B). The C<sup>ε</sup> atom of Met245 also rotated by ~90° about the C<sup>γ</sup>–S<sup>δ</sup> bond. These side chain movements are the only significant change in the protein structure to occur upon DMG binding, as compared with the other complexes.

## DISCUSSION

**Anionic Flavin Ring Forms.** MSOX stabilizes the anionic form of the oxidized flavin ( $pK_a = 8.3$  versus 10.4 with free FAD) (16) and forms a thermodynamically stable flavin radical. MSOX stabilizes the anionic form of the flavin radical ( $pK_a < 6$  versus  $pK_a = 8.3$  with free flavin) (23), as judged by the observed quantitative conversion to the anionic radical at pH 7. MSOX forms a sulfite complex at pH 7, but complex formation is very slow. Studies with *N*-methyltryptophan oxidase (MTOX), the closest known homologue of MSOX (43% sequence identity), show that reactivity with sulfite is enhanced at lower pH values, but MSOX is unstable at pH < 7. A moderately stable sulfite complex is formed with MTOX at pH 6.0 ( $K_d = 1.7$  mM). The rate of complex formation is, however, extremely slow, even at this pH ( $k_f = 5.4 \times 10^{-3} \text{ M}^{-1} \text{ s}^{-1}$ ).<sup>3</sup> The observed rate is 10<sup>2</sup>- to 10<sup>7</sup>-fold slower than values obtained with other flavoprotein oxidases (24), suggesting that there may be a significant

kinetic barrier against complex formation with *N*-methyltryptophan oxidase and other members of the MSOX family.

Formation of a flavin•sulfite complex, the anionic oxidized flavin, or the anionic flavin radical results in the development of negative charge at the N(1)–C(2)–O locus of the flavin ring (Scheme 1). The flavin ring in MSOX is located in a highly basic environment that contains seven basic residues and various neutral residues but no acidic residues (7). The  $\epsilon$ -amino group of Lys348 is 2.8 Å away, and hydrogen bonds to the C(2) carbonyl oxygen of the flavin ring. The positive end of a helix dipole ( $\alpha$ F4) points toward the same carbonyl oxygen. Structural studies with various other flavoprotein oxidases show the presence of similar positive charge(s) near the N(1)–C(2)–O locus of the flavin (25–28). Formation of an anionic radical and a sulfite complex are properties characteristically observed with flavoprotein oxidases (19, 29) and generally not with other classes of flavoenzymes, although certain exceptions have been reported, such as flavocytochrome *b*<sub>2</sub> (30, 31). The importance of a positive charge near the C(2) carbonyl in stabilizing the sulfite complex and the anionic radical has been functionally verified in mutation studies with lactate oxidase (32). This positive charge is probably not a key feature in stabilizing the anionic oxidized flavin. A decreased  $pK_a$  for oxidized flavin ionization is not a general characteristic of flavoprotein oxidases but has been observed with several other oxidase enzymes (glycolate oxidase, nitroalkane oxidase, long-chain 2-hydroxy acid oxidase) that exhibit  $pK_a$  values in the range of 6.4 to 8.4 (33–36). Studies with glycolate oxidase show that the anionic oxidized flavin is stabilized by hydrogen bonding between the C(4) carbonyl oxygen and the hydroxyl group of Tyr129 (37). The C(4) carbonyl oxygen in MSOX forms hydrogen bonds with a water molecule and the amide nitrogen of Ile50 (7).

**Substrate Binding Determinants.** The carboxyl group of sarcosine is essential since no binding is observed with simple amines. This is consistent with crystallographic studies that show that the carboxylate group in substrate analogues (MTA, PCA, DMG, MSEA, MTEA) forms hydrogen bonds to the side chains of two basic residues, Lys348 and Arg52, an interaction associated with the movement of a loop region that closes up the active site cleft (7). The amino group of sarcosine is not essential, but binding affinity depends on the nature of the substitution (vide infra). MSOX forms complexes with dimethylthioacetate [(CH<sub>3</sub>)<sub>2</sub>S<sup>+</sup>CH<sub>2</sub>CO<sub>2</sub><sup>–</sup>] and DMG [(CH<sub>3</sub>)<sub>2</sub>NH<sup>+</sup>CH<sub>2</sub>CO<sub>2</sub><sup>–</sup>]

that are spectroscopically and thermodynamically ( $K_d = 20.5$  and  $17.4$  mM, respectively) very similar, suggesting that amino acids are bound as zwitterions, a conclusion fully supported by the crystal structure of the MSOX·DMG complex. The methyl group of sarcosine is not essential, since binding is observed when the methyl group in  $\text{CH}_3\text{XCH}_2\text{CO}_2^-$  is replaced by hydrogen, but the methyl group does contribute to binding affinity. The methyl group contribution may reflect van der Waals interactions with atoms of the flavin ring, His269, Tyr317, and Tyr254 (Figure 8B). The observed contribution varied from  $-3.79$  to  $-0.65$  kcal/mol, depending on the nature of the heteroatom (Table 3), and appeared to be inversely correlated with heteroatom electron density ( $\text{NH}_2^+ > \text{O} > \text{S}$ ) (assuming that sarcosine and glycine bind as zwitterions). Interaction of MSOX with the methyl group is consistent with Raman difference spectra obtained for complexes with  $\text{CH}_3\text{XCH}_2\text{CO}_2^-$  when  $\text{X} = \text{S}$  or Se. The observed spectra exhibit greatly enhanced symmetric bending of the methyl group as compared with the free ligands.<sup>6</sup> PCA, the aromatic analogue of L-proline, forms a complex with MSOX ( $\Delta G_a = -3.91$  kcal/mol) that is  $3.2$  kcal more stable than the complex formed with L-proline ( $\Delta G_a = -0.74$  kcal/mol), an alternate substrate for MSOX (9). PCA and MTA are nearly planar when bound to MSOX (7). Steric factors may account for the weaker binding of L-proline since a significant barrier to planarity is expected for the pyrrolidine ring in L-proline, as judged by results reported for cyclopentane ( $\Delta G = 5.2$  kcal/mol) (38).

**Donor- $\pi$  Interactions.** A progressive increase in binding affinity is observed for the series of complexes formed with MSOX and  $\text{CH}_3\text{XCH}_2\text{CO}_2^-$  when  $\text{X} = \text{CH}_2$ , O, S, Se, or Te (Table 1). The results obtained when  $\text{X} = \text{CH}_2$ , O, or S parallel those obtained for a series of model flavin complexes formed with a analogous set of ligands (39) (Table 4). The observed effect on binding energy in the model flavin complexes has been attributed to differences in the strength of donor- $\pi$  interactions between the ligand and the flavin ring. Donor- $\pi$  interactions are electronic interactions between an electron-rich donor atom and an electron-deficient  $\pi$  system whose strength appears to correlate with the polarizability of the donor atom (39). The larger contribution to binding energy estimated for donor- $\pi$  interactions when  $\text{X} = \text{S}$  or O with MSOX ( $\Delta\Delta G_a = -2.26$  or  $-0.84$  kcal/mol, respectively) versus the model flavin system ( $\Delta\Delta G_a = -0.95$  or  $-0.49$  kcal/mol, respectively) may reflect, in part, a more electron-deficient flavin in the enzyme. The modest increase in the strength of donor- $\pi$  interactions estimated for the higher group VIa elements ( $\text{X} = \text{Se}$ , Te) might suggest that the contribution from polarization effects may reach a limiting value. However, the structures of the MSOX complexes with MSEA ( $\text{X} = \text{Se}$ ) and MTEA ( $\text{X} = \text{Te}$ ) show that these ligands bind in two conformations. The occupancy of the conformation superimposable with MTA ( $\text{X} = \text{S}$ ) is estimated at 65% when  $\text{X} = \text{Se}$  and 50% when  $\text{X} = \text{Te}$ . The larger size of the higher group VIa elements may introduce steric factors that favor an alternate binding mode and lead us to underestimate the contribution from donor- $\pi$  interactions to binding energy. It will be of interest to see whether larger increases in the magnitude of donor- $\pi$

interactions are observed with Se and Te derivatives in model systems where steric factors do not intervene.

**Charge-Transfer Interactions.** Charge-transfer complexes are formed with MSOX and sarcosine analogues ( $\text{CH}_3\text{XCH}_2\text{CO}_2^-$ ,  $\text{X} = \text{S}$ , Se, Te), aromatic heterocyclic carboxylates containing a five-membered ring ( $\text{X} = \text{NH}$ , O, S), and thioglycolate ( $\text{HSCH}_2\text{CO}_2^-$ ). PCA and MTA lie parallel to and about  $3.1$  Å above the *re* face of the flavin ring when bound to MSOX (7). One of the two conformations observed with MSEA and MTEA is superimposable with the binding mode observed for MTA. This close stacking probably facilitates the charge-transfer interactions observed with these and other similar ligands. The MSOX charge-transfer complexes are likely to involve the electron-deficient flavin and ligand as acceptor and donor, respectively. Charge-transfer complexes are characterized by the appearance of a new absorption band unique to the complex. In the case of complexes formed with the same acceptor and different donors, the energy of the charge-transfer band should be linearly correlated with the one-electron reduction potential ( $E^\circ$ ) of the donor. An excellent linear correlation ( $r^2 = 0.998$ ) is observed between the energy of the charge-transfer bands for the complexes formed with  $\text{CH}_3\text{XCH}_2\text{CO}_2^-$  and the one-electron reduction potentials of the ligands, as estimated by  $E^\circ$  values reported for a series of diaryl chalcogenides [ $(\text{C}_6\text{H}_5)_2\text{X}^{+}/(\text{C}_6\text{H}_5)_2\text{X}$ ] (40) (Figure 6, inset). Ionization potentials (IP) have been measured for aromatic heterocyclic ring compounds ( $\text{C}_4\text{H}_4\text{X}^{+}/\text{C}_4\text{H}_4\text{X}$ ,  $\text{X} = \text{NH}$ , O, S) (41), but the corresponding  $E^\circ$  values are unknown. Although IP values cannot be used to predict absolute  $E^\circ$  values, the data can provide an estimate of relative  $E^\circ$  values, assuming that hydration effects are similar with different heteroatoms. A very good linear correlation ( $r^2 = 0.97$ ) is found between the energy of the charge-transfer bands for complexes formed with aromatic heterocyclic carboxylates and the IP values reported for the corresponding heterocyclic rings (Figure 7C). It may, however, be argued that more points are needed to justify a linear relationship in view of the similar values observed when  $\text{X} = \text{S}$  or O. The charge-transfer band of the complex formed with  $\text{HSCH}_2\text{CO}_2^-$  ( $\lambda_{\text{max}} = 508$  nm) is higher in energy than observed with  $\text{CH}_3\text{SCH}_2\text{CO}_2^-$  ( $\lambda_{\text{max}} = 532$  nm). This result is opposite to that expected based on  $E^\circ$  values reported for thioethers [ $(\text{CH}_3)_2\text{S}^{+}/(\text{CH}_3)_2\text{S}$ ,  $E^\circ = 1.66$  V] (42) versus thiols or thiolate anions [ $\text{CH}_3\text{S}^{+}\text{H}/\text{CH}_3\text{SH}$ ,  $E^\circ = 1.35$  V;  $\text{CH}_3\text{S}^{\bullet}/\text{CH}_3\text{S}^-$ ,  $E^\circ = 0.78$  V (43)]. The basis for this discrepancy is unclear.

**Concluding Remarks.** This paper describes, for the first time, the basic biochemical and biophysical properties of MSOX, a member of a newly recognized family of eukaryotic and prokaryotic amine oxidases. MSOX is the only member with a known structure and, as such, serves as a paradigm for other enzymes in this family. The results provide important information for future mechanistic and structure-function studies. This paper documents the stabilization of anionic flavin ring forms and provides an in-depth thermodynamic characterization of substrate binding determinants, including identification of the protonation state of the substrate amino group in the enzyme-substrate complex. This information will serve as a basis for mutagenesis studies to more precisely define the residues responsible for the observed stabilization of anionic flavin ring forms

<sup>6</sup> Y. Zheng, M. A. Wagner, M. S. Jorns, and P. Carey, unpublished results.



that can be correlated with the basic active site environment of MSOX. Knowledge of flavin ionization constants should prove useful in the interpretation of pH activity profiles.

## ACKNOWLEDGMENT

We thank Dr. Louis Silks [National Stable Isotope Resource at Los Alamos and NIH Supported Resource (RR02231)] for his generous gifts of methylselenoacetate and methyltelluroacetate and Dr. George Markham (Fox Chase Cancer Center) for his generous gift of dimethylthioacetate. We thank Drs. David Armstrong (University of Calgary), Vincent Rotello (University of Massachusetts), and Gabor Merenyi (Royal Institute of Technology) for helpful advice and useful discussions.

## REFERENCES

- Kvalnes-Krick, K., and Jorns, M. S. (1991) in *Chemistry and Biochemistry of Flavoenzymes* (Muller, F., Ed.) pp 425–435, CRC Press, Boca Raton.
- Willie, A., Edmondson, D. E., and Jorns, M. S. (1996) *Biochemistry* 35, 5292–5299.
- Wagner, M. A., Khanna, P., and Jorns, M. S. (1999) *Biochemistry* 38, 5588–5595.
- Chlumsky, L. J., Zhang, L., and Jorns, M. S. (1995) *J. Biol. Chem.* 270, 18252–18259.
- Reuber, B. E., Karl, C., Reimann, S. A., Mihalik, S. J., and Dodt, G. (1997) *J. Biol. Chem.* 272, 6766–6776.
- Chlumsky, L. J., Sturgess, A. W., Nieves, E., and Jorns, M. S. (1998) *Biochemistry* 37, 2089–2095.
- Trickey, P., Wagner, M. A., Jorns, M. S., and Mathews, F. S. (1999) *Structure* 7, 331–345.
- Ashton, W. T., Brown, R., Jacobson, F., and Walsh, C. (1979) *J. Am. Chem. Soc.* 101, 4419–4420.
- Wagner, M. A., and Jorns, M. S. (2000) *Biochemistry* 39, 8825–8829.
- Otwinowski, Z., and Minor, W. (1997) *Methods Enzymol.* 276, 307–326.
- Brünger, A. T., Adams, P. D., Clore, G. M., DeLano, W. L., Gros, P., Grosse-Kunstleve, R. W., Jiang, J. S., Kuszewski, J., Nilges, M., Pannu, N. S., Read, R. J., Rice, L. M., Simonson, T., and Warren, G. L. (1998) *Acta Crystallogr. D* 54, 905–921.
- Kleywegt, G. J., and Brünger, A. T. (1996) *Structure* 4, 897–904.
- Jiang, J.-S., and Brünger, A. T. (1994) *J. Mol. Biol.* 243, 100–115.
- Allen, F. H., and Kennard, O. (1993) *Chem. Des. Autom. News* 8, 1–31.
- Roussel, A., and Cambillau, C. (1991) *TURBO-FRODO in Silicon Graphics Geometry Partners Directory* 86, Silicon Graphics, Mountain View, CA.
- Massey, V., and Ganther, H. (1965) *Biochemistry* 4, 1161–1173.
- Massey, V., and Hemmerich, P. (1978) *Biochemistry* 17, 9–17.
- Stankovich, M., and Fox, B. (1983) *Biochemistry* 22, 4466–4472.
- Massey, V., Muller, F., Feldberg, R., Schuman, M., Sullivan, P. A., Howell, L. G., Mayhew, S. G., Matthews, R. G., and Foust, G. P. (1969) *J. Biol. Chem.* 244, 3999–4006.
- Thompson, M. J., Mekhelfia, A., Jakeman, D. L., Phillips, S. E. V., Phillips, K., Porter, J., and Blackburn, G. M. (1996) *Chem. Commun.* 791–792.
- Ramachandran, G. N., and Sasisekharan, V. (1968) *Adv. Protein Chem.* 23, 283–438.
- Laskowski, R. A., MacArthur, M. W., Moss, D. S., and Thornton, J. M. (1993) *J. App. Crystallogr.* 26, 283–291.
- Muller, F. (1991) in *Chemistry and Biochemistry of Flavoenzymes* (Muller, F., Ed.) pp 2–71, CRC Press, Boca Raton.
- Parsonage, D., Luba, J., Mallett, T. C., and Claiborne, A. (1998) *J. Biol. Chem.* 273, 23812–23822.
- Mattevi, A., Vanoni, M. A., Todone, F., Rizzi, M., Teplyakov, A., Coda, A., Bolognesi, M., and Curti, B. (1996) *Proc. Natl. Acad. Sci. U.S.A.* 93, 7496–7501.
- Mattevi, A., Fraaije, M. W., Mozzarelli, A., Olivi, L., Coda, A., and Vanberkel, W. J. H. (1997) *Structure* 5, 907–920.
- Lindqvist, Y., and Branden, C. I. (1989) *J. Biol. Chem.* 264, 3624–3628.
- Vrielink, A., Lloyd, L. F., and Blow, D. M. (1991) *J. Mol. Biol.* 219, 533–554.
- Massey, V., and Palmer, G. (1966) *Biochemistry* 5, 3181–3189.
- Capeillere-Blandin, C., Bray, R. C., Iwatsubo, M., and Labeyrie, F. (1975) *Eur. J. Biochem.* 54, 549–566.
- Lederer, F. (1978) *Eur. J. Biochem.* 88, 425–431.
- Muh, U., Massey, V., and Williams, C. H. (1994) *J. Biol. Chem.* 269, 7982–7988.
- Schuman, M., and Massey, V. (1972) *Biochim. Biophys. Acta* 227, 500–520.
- Macheroux, P., Massey, V., Thiele, D. J., and Volokita, M. (1991) *Biochemistry* 30, 4612–4619.
- Gadda, G., and Fitzpatrick, P. F. (1998) *Biochemistry* 37, 6154–6164.
- Belmouden, A., and Lederer, F. (1996) *Eur. J. Biochem.* 238, 790–798.
- Macheroux, P., Kieweg, V., Massey, V., Soderlind, E., Stenberg, K., and Lindqvist, Y. (1993) *Eur. J. Biochem.* 213, 1047–1054.
- Carreira, L. A., Jiang, G. J., Person, W. B., and Willis, J. N. (1972) *J. Chem. Phys.* 56, 1440–1443.
- Breinlinger, E. C., Keenan, C. J., and Rotello, V. M. (1998) *J. Am. Chem. Soc.* 120, 8606–8609.
- Engman, L., Lind, J., and Merenyi, G. (1994) *J. Phys. Chem.* 98, 3174–3182.
- Lias, S. G. (1998) in *NIST Chemistry WebBook, NIST Standard Reference, Database No. 69* (Mallard, W. G., and Linstrom, P. J., Eds.) National Institute of Standards and Technology, Gaithersburg, MD. <http://webbook.nist.gov>
- Merenyi, G., and Lind, J. (1996) *J. Phys. Chem.* 100, 8875–8881.
- Armstrong, D. A. (1999) in *S-Centered Radicals* (Alfassi, Z. B., Ed.) pp 27–61, John Wiley and Sons, New York.

BI000349Z